

## Research Article

# Research on Multifactor Analysis and Quantitative Evaluation Method of Rockburst Risk in Coal Mines

Weisheng Du <sup>1,2</sup> Haitao Li <sup>2</sup> Qingxin Qi,<sup>2</sup> Weiyu Zheng,<sup>2</sup> and Sensen Yang<sup>2</sup>

<sup>1</sup>State Key Laboratory of Hydrosience and Engineering, Tsinghua University, Beijing 100084, China

<sup>2</sup>Deep Mining and Rock Burst Research Branch, Chinese Institute of Coal Science, Beijing 100013, China

Correspondence should be addressed to Haitao Li; [catchyou@qq.com](mailto:catchyou@qq.com)

Received 24 June 2022; Revised 27 September 2022; Accepted 8 October 2022; Published 8 November 2022

Academic Editor: Shaofeng Wang

Copyright © 2022 Weisheng Du et al. Exclusive Licensee GeoScienceWorld. Distributed under a Creative Commons Attribution License (CC BY 4.0).

The prevention of rockbursts is significant to ensure mining safety in deep coal mines. The multifactor analysis and a new quantitative evaluation method for rockbursts in coal mines are proposed in this study. In the aspect of rockburst analysis, a multifactor system of rockburst risk based on the material, stress, and large-scale geological structure is proposed. The factors influencing rockbursts in coal mines are analyzed by numerical simulations. Based on a standard mining model, three comparative models considering the rockburst tendency, high stress, and geological structure are established. The distribution of maximum principal stress and plastic zone during the mining process is compared. The reasons why these three types of factors are liable to trigger rockbursts lie in generating high-stress zones in surrounding rock masses. In the aspect of quantitative evaluation, the monitored microseismic signal is selected as the key indicator, and the daily frequency of microseisms is analyzed. A normal distribution function based on the daily frequency of microseisms is established. The interval of daily frequency of microseisms is set to judge whether the microseismic frequency is abnormal and then determine the rockburst risk of coal mines. Considering the results of multifactor analysis, it is proposed that the monitoring system combining microseisms with stress is the direction to accurately and quantitatively evaluate the rockburst risk in the future. This study makes specific explorations in the quantitative evaluation of rockburst risk in coal mines.

## 1. Introduction

The rockburst in coal mines is the dynamic phenomenon of sudden and severe destruction of rock masses around roadways or working faces due to the instantaneous release of elastic energy [1]. This dynamic phenomenon often accompanies coal and rock mass throwing, loud noises, and airwaves, which has become one of the significant threats to the safe mining of coal mines [2, 3]. On May 12, 2014, a rockburst accident occurred while recovering coal pillars in a mine in Boone County, West Virginia, USA, killing two miners [4]. Coincidentally, another rockburst accident occurred in Longyun Coal Company in Shandong Province in China, causing 22 people to be trapped underground on October 20, 2018 [5]. The longwall mining method is widely used in deep coal mines in China, which results in hundreds of thousands or even millions of cubic meters of mining space. The scope of underground space excavation in coal

mines is beyond that of any other underground engineering. The longwall mining method with large space and rapid excavation would cause strong mining disturbance to surrounding rock, which easily leads to rockbursts in coal mines. According to statistics, rockbursts have happened in many coal mines in China; whether the geological structure is simple or complex, the coal seam is thin or extra thick, the dip angle of coal strata is horizontal or steep, and the roof is conglomerate, sandstone, limestone, or shale. There are many factors affecting rockbursts, such as the mechanical properties of rock strata, the influence of mining activities, the stress environment, and geological structure, and so on. Researchers have analyzed the mechanism of rockbursts from different aspects. Cai et al. [6] supported that the rockburst was caused by coupled static-dynamic stress, while the static stress was the abutment pressure caused by mining, and dynamic stress included the dynamic stress caused by vibration and

impact. Rehbock-Sander and Jesel [7] deemed that it was easy to cause sliding rockburst when the excavation passed through the fault, and this viewpoint was confirmed by tunnel construction engineering. Zhao et al. [3] believed that the existence of coal pillars could cause strong stress concentration when mining irregular-shaped coal seams, which could lead to rockbursts in coal mines. Zhu et al. [8] deemed that a large-scale rockburst could occur when mining deep remnant island longwall panels, resulting in a very violent energy release.

The current research on rockburst in coal mines mainly focuses on risk evaluation and early warning and prevention of rockburst [8–10]. The studies on early warning of rockburst are extended from the laboratory to engineering sites. In the aspect of rock mechanics experiment, the precursor information of rock specimen failure during the loading process is mainly studied by employing acoustic emission, thermal infrared, and electromagnetic radiation [11–14]. In terms of rock engineering, early warning of rockbursts in coal mines is mainly realized by microseismic monitoring, rock noise, electromagnetic radiation, and drilling cutting method [15–18]. The evaluation of rockburst risk is the prerequisite for early warning. The State Administration of Work Safety of China stipulates that all mines with solid vibration, instantaneous bottom drum, rock ejection, and other dynamic phenomena must be subjected to rockburst risk evaluation, which shows the significance of the rockburst risk evaluation. Plenty of efforts have been made in terms of rockburst risk evaluation. In general, there are two types of qualitative and quantitative evaluation methods. Many complex calculations do not characterize qualitative evaluation, but the elements and information are required to be as comprehensive as possible [19]. The existing qualitative evaluation methods of rockburst risk mainly include engineering analogy and multifactor superposition. The typical studies on the qualitative evaluation of rockburst risks are as follows. Qi et al. [20] analyzed the deficiencies in evaluating the rockburst risk by dynamic failure time, rockburst energy index, and elastic energy index, and suggested using the uniaxial compressive strength of coal as a new index to evaluate the rockburst risk of coal seams. Zhai et al. [21] proposed a comprehensive classification method for rockburst combining eight external force sources and ten typical surrounding rock structures. The evaluation of rockbursts is analyzed and optimized based on the classification. Konicek and Schreiber [22] analyzed the microseismic activity recorded during longwall mining and used these statistical microseismic data to evaluate the risk of rockbursts in coal mines roughly.

In terms of quantitative evaluation, Chen et al. [23] studied the relationship between rockburst radiation energy and intensity, chose energy as the evaluation index of rockburst intensity classification, and proposed a new quantitative classification method of rockburst intensity. Zhu et al. [24] calculated the relationship between mining depth, ground stress, active faults, other geological environmental factors, and rockburst, and established a rockburst risk evaluation method with the help of a fuzzy evaluation method and analytic hierarchy process. Wang et al. [25] established a con-

ceptual model to explain the possibility of rockburst and selected nine typical rockburst indicators to evaluate the rockburst potential. Zhang [26] proposed a rockburst risk evaluation method based on BP neural network, using a PSO algorithm to optimize connection weights to evaluate the problem of slow convergence of the BP network. Microseismic monitoring is a good method to evaluate rockbursts. Yu et al. [27] proposed a fractal dimension related to microseisms for immediate rockburst warning and analyzed the distribution range and evolution of energy fractal dimension during rockbursts; the results were used to guide the rockburst prediction. Feng et al. [28] monitored the microseismic characteristics of deep-buried tunnels in alternate soft and hard strata and found six microseismic threshold values that can be used to warn rockbursts in different lithology based on 58 cases.

The above studies have promoted the development of rockburst risk evaluation in coal mines. However, the existing evaluation methods have the following deficiencies. First, the influencing factors are not fully classified, and the mechanism of these factors affecting rockburst has not been systematically compared and analyzed. Second, the existing quantitative evaluation methods of rockbursts in coal mines are not simple enough. The relationship between monitoring signals and rockburst risk is not elaborated, and the monitoring results of low microseismic frequency are often ignored. In this study, the main control factors of rockbursts in coal mines are systematically analyzed. How these factors affect rockburst is simulated in a uniform model. It is pointed out that the core of rockbursts is stress concentration and energy release. Accordingly, a normal distribution model based on the daily frequency of microseisms is established to evaluate the risk of rockburst quantitatively. Then the role of the three factors in inducing rockbursts and the expectation of rockbursts evaluation are discussed. This study is helpful to promote the multifactor analysis and quantitative evaluation of rockbursts in coal mines.

## 2. Multifactor Analysis of Rockbursts in Coal Mines

The rockburst in coal mines is a physical process affected by multiple factors. As a dynamic disaster, it should meet the following primary conditions: (1) the mechanical properties of rock materials can ensure that energy is stored as elastic deformation energy; (2) there is a mechanical environment with stress concentration and disturbance to ensure the continuous supply of energy; (3) there is a particular structure that constrains a large amount of elastic energy in the rock masses and causes a large amount of elastic energy to be released suddenly after the rock mass is destroyed. Therefore, the factors that induce rockbursts in coal mines are divided into three categories: material, stress, and structure. The three types of factors interact and form the fundamental inducing factors of rockbursts in coal mines.

*2.1. Material Factors of the Rock Medium.* Material factors refer to the related factors that bring differences in the basic mechanical properties and are difficult to change, such as

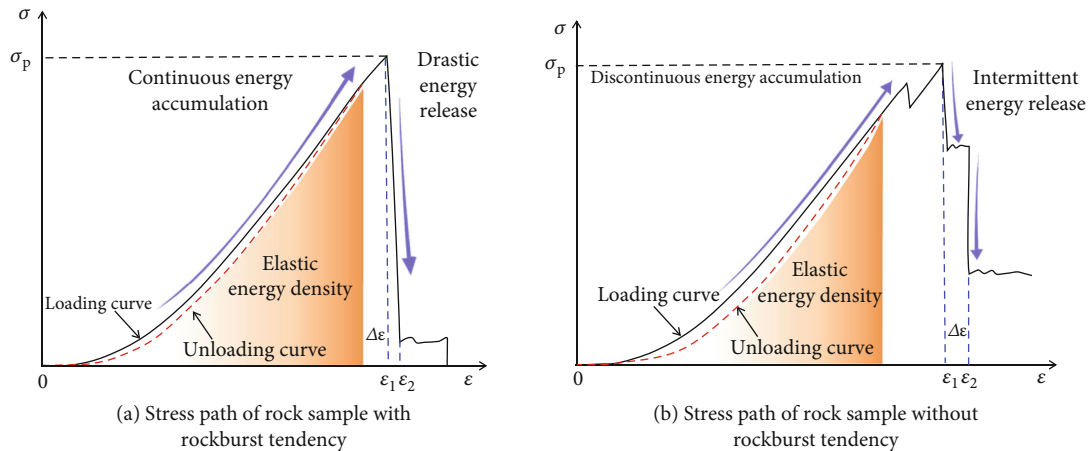


FIGURE 1: Different energy development modes of the two rock materials.

basic substance types, dislocation structures, and composition distribution. There are three most widely-used material indicators to measure rockburst tendency: elastic energy index, rockburst energy index, and dynamic failure time. These three indicators define the nature of the material that induces rockbursts in coal mines from the energy point of view; that is, the material can store a large amount of elastic energy and release energy in a relatively short time. That is, rock materials are required to accumulate energy stably and release energy sharply [29, 30].

The stress evolution process of different materials during uniaxial compression is shown in Figure 1. The uniaxial compression stress-strain curve of rock with rockburst tendency is exhibited in Figure 1(a). The area enclosed by the loading curve and the strain axis is the energy density input to the specimen; the area enclosed by the unloading curve and the strain axis is the elastic deformation energy density released during the unloading process. It can be found that for this type of rock sample, most input energy is stored in the form of elastic deformation. As the specimen is continuously loaded, the energy stored in the specimen continues to increase steadily. The sample is severely damaged until it reaches the peak strain  $\sigma_p$ . The stress drops after the peak is remarkable; the strain  $\Delta\epsilon$  experienced is very small, and the stored elastic energy of the specimen can be violently released. Figure 1(b) shows the loading process of a specimen with no rockburst tendency. The energy evolution process can explain why this type of rock sample has no rockburst tendency: the large gap between the loading and unloading curves of the sample indicates that more energy is dissipated during the loading process; there is a stress drop before the peak, indicating that the energy accumulation is not continuous; the occurrence of multiple stress drops after the peak indicates that the energy release process takes a long time.

## 2.2. Stress Factors of Rock Masses in Mining Engineering.

Stress factors refer to a series of mechanical behaviors such as deformation and failure of the rock masses, such as the stress caused by the suspended roof of the rock layer acting on the coal masses and the stress concentration after the

redistribution caused by mining [31–33]. Combined with the remarkable engineering characteristics of underground coal mining, it is revealed why rockbursts in coal mines are easily induced during coal mining from stress factors.

Figure 2 is a schematic figure of the mechanism of rockbursts in coal mines occurring in a roadway under the combined action of dynamic and static loads. In Figure 2, the rock surrounding the roadway is subjected initially to the static load  $\sigma_s$  imposed by the overlying rock layer. Mining activities lead to a thick and hard rock layer on the roof suddenly fracturing, generating a dynamic load  $\sigma_d$ . This dynamic load is superimposed on the initial static load, and the surrounding rock of the roadway bears a combined dynamic and static load. In this process, the static load plays the role of early energy accumulation, while the dynamic load plays the role of the disturbance and contributes to the massive release of energy. It is worth mentioning that whether static load or dynamic load has a more significant role in inducing rockbursts in coal mines has not yet been explained clearly.

**2.3. Large-Scale Geological Structure Factors.** Structure factors refer to natural or man-made factors that can destroy the uniformity and continuity of the media and their spatial systems, such as the structure plane system in the coal and rock media, geological structure, and coal pillars formed by mining activities. The geological environment of underground coal mining is complex. In addition to the original natural geological structure of faults [34], collapsed columns, and folds, the newly formed engineering structures such as large-area suspended roofs and isolated working faces formed during the mining process cannot be ignored [35–37].

A case of a coal pillar rockburst is taken as an example. As shown in Figure 3, the influence of large-scale structural factors on the rockburst in a coal mine is analyzed. First, the cutting of the reverse fault has a stress barrier effect, which puts the top plate of the fault zone in a low-stress state and the bottom plate in a state of stress concentration. When the coal seam is mined near the fault, the mining process triggers the fault activation. The bottom plate in a state of

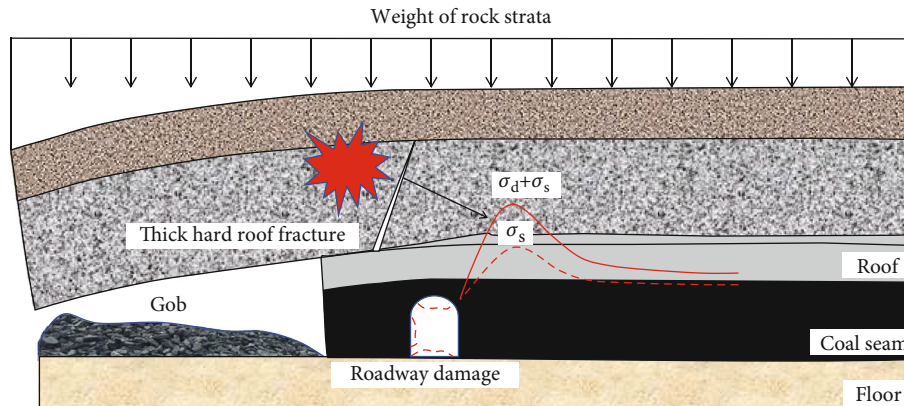


FIGURE 2: Mechanism of rockbursts in coal mines in the roadway induced by stress factors.

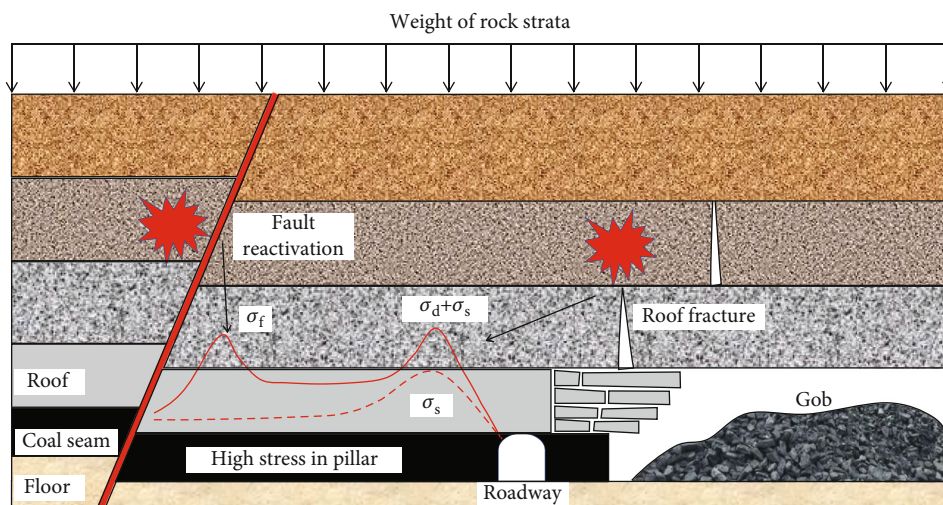


FIGURE 3: Mechanism of coal pillar rockburst induced by fault structure.

stress concentration generates activation stress  $\sigma_f$  after fault activation. Under the superposition of the mining stress  $\sigma_d$ , the overlying static load  $\sigma_s$  and the fault activation stress  $\sigma_f$ , high stresses are formed in the coal pillars between the fault and the roadway, which can easily cause the coal pillar rockburst.

### 3. Numerical Simulation of Multifactor Analysis of Rockburst in Coal Mines

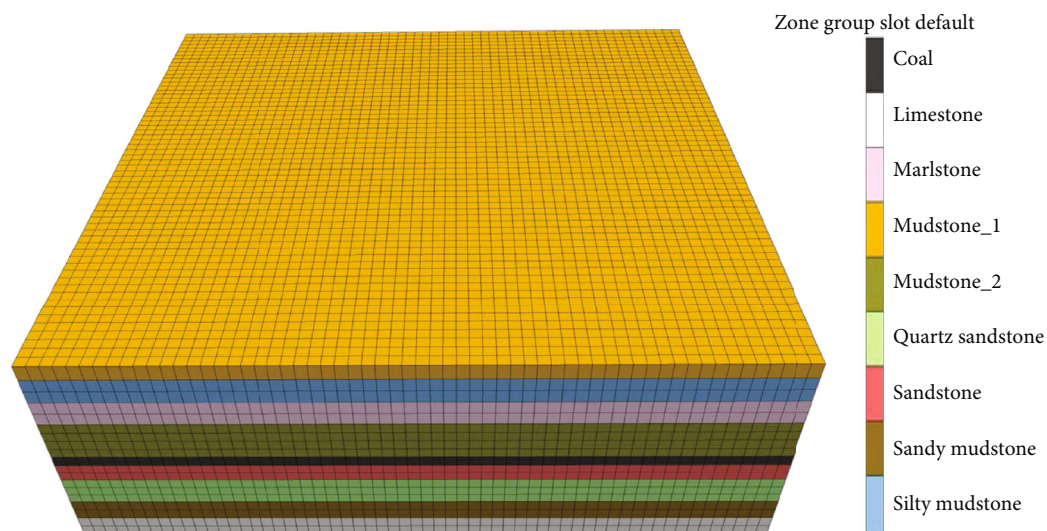
Four numerical models of engineering scales are established in this section, and the simulation analysis of multifactors affecting the rockbursts in coal mines in Section 2 is carried out. The distribution of stress and plastic zone in the coal seam mining process is compared under the action of different factors.

#### 3.1. Establishment and Simulation Analysis of the Standard Mining Model

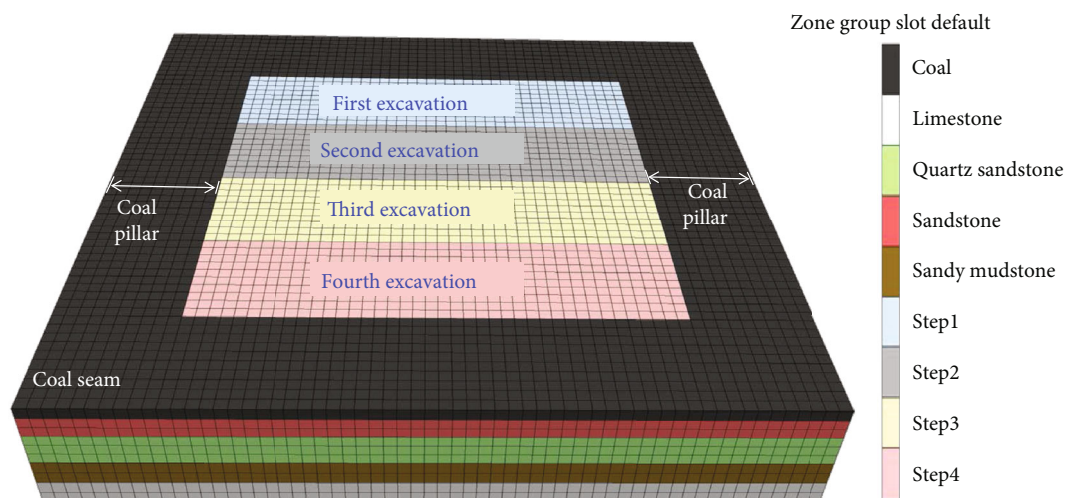
**3.1.1. Establishment of the Standard Mining Model.** A standard mining model should be established for comparative analysis with the subsequent influence of the different

factors. In this standard model, the material of each rock formation has no rockburst tendency, the model is in a low-stress environment, and the model does not contain geological structures. In this engineering model, it is worth paying attention to the mechanical behavior around the mining space, so the established model only includes the coal seam and the area within 100 m of the roof and floor.

Figure 4 shows the established standard mining model. The length, width, and height of the model size are 300, 300, and 100 m, respectively. The coal mining method is the long wall mining method. The length of the working face is 200 m with coal pillars of 50 m around. There are 9 rock formations in the model from bottom to top, namely, limestone, sandy mudstone, quartz sandstone, sandstone, coal, mudstone\_2, marlstone, silty mudstone, and mudstone\_1. The overlying rock strata of the model are 300 m, and the density of the rock is taken as  $2500 \text{ kg/m}^3$ , which is applied to the top of the model by its weight. The simulation software is FLAC3D 6.0, and the failure criterion is the M-C Criterion. The mechanical parameters of the rock formations are shown in Table 1 [38]. During the simulation process, the distribution of stress and plastic zone around the mining



(a) Rock formations of the standard mining model

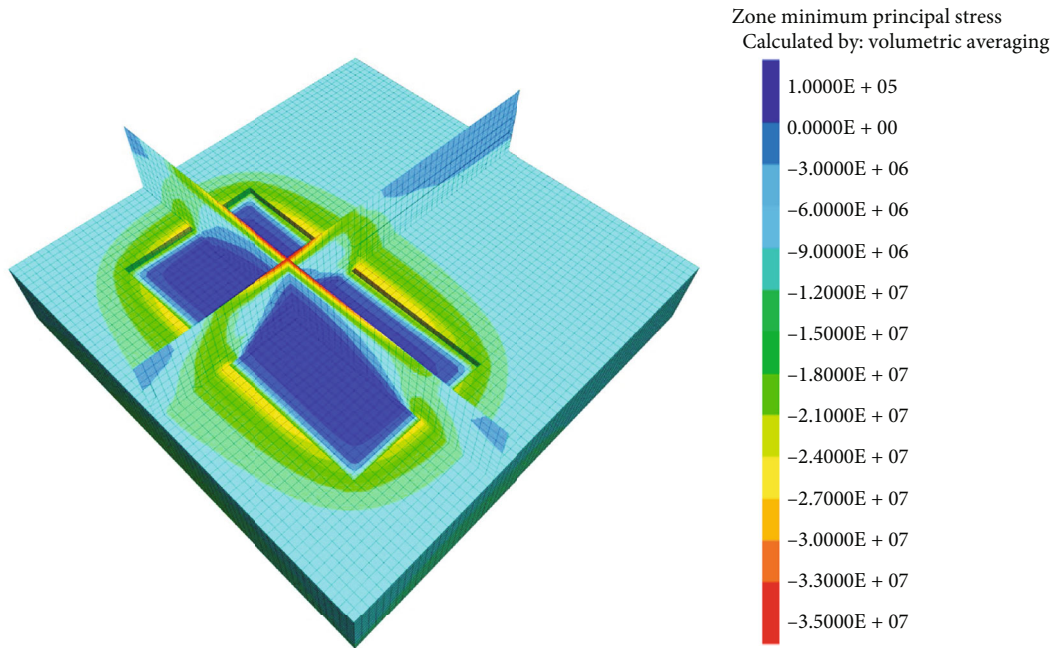


(b) Coal seam and excavation position of the mining model

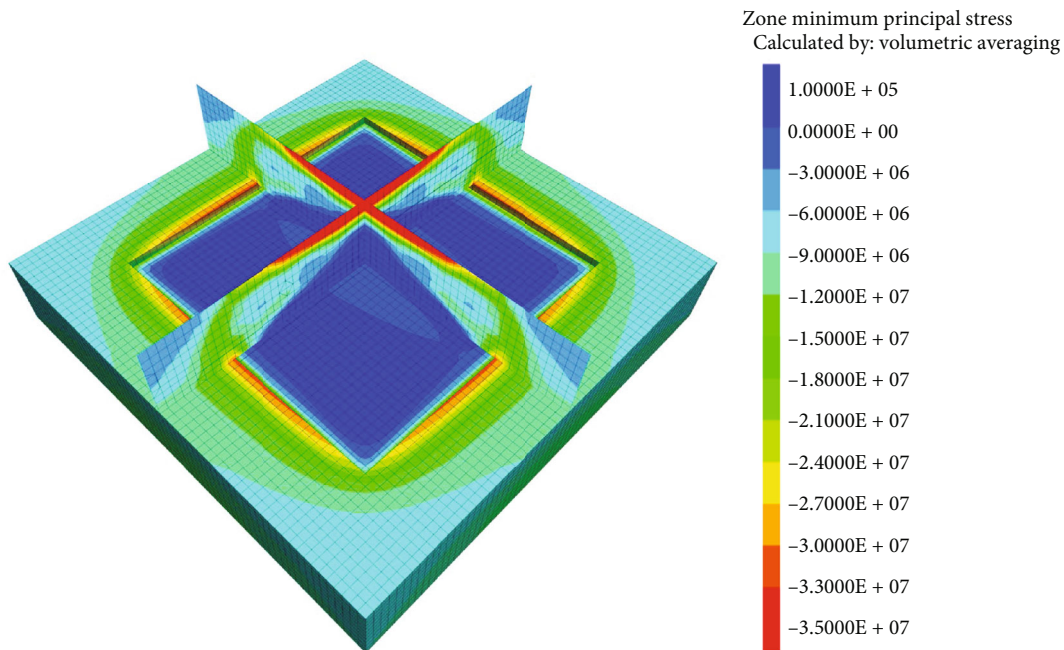
FIGURE 4: Established standard mining model.

TABLE 1: Rock formation parameters selected in the standard mining model.

Lithology	Thickness/ m	Bulk modulus/ GPa	Shear modulus/ GPa	Cohesive force/ MPa	Tensile strength/ MPa	Friction angle/°	Density kg/m <sup>3</sup>
Limestone	7.0	8.95	5.68	4	1.75	38	2738
Sandy mudstone	12.0	1.68	1.08	3	0.71	24	2723
Quartz sandstone	12.0	1.57	1.06	3	1.83	32	2570
Sandstone	19.0	2.23	1.74	4.1	0.93	43	2839
Coal	5.0	1.41	0.45	1	0.8	25	1400
Mudstone_2	9.0	1.76	0.61	2.6	0.5	30	2762
Marlstone	14.0	8.95	5.68	4	1.75	38	2728
Silty mudstone	11.0	2.58	1.23	3.6	0.73	36	2729
Mudstone_1	11.0	1.76	0.61	2.6	0.5	30	2762



(a) Coal seam excavation for 100 m



(b) Coal seam excavation for 200 m

FIGURE 5: Distribution of the maximum principal stress in the standard model.

space is calculated after excavation of 50, 100, 150, and 200 m, respectively.

**3.1.2. Stress Distribution in the Standard Mining Model.** Mining activities would cause stress redistribution in the surrounding rock near the working face, so analyzing the stress distribution after mining is the basis for analyzing the mechanical behavior of the surrounding rock. This study shows the distribution of the maximum principal stress

around the mining space when the working face is excavated for 100 and 200 m. It should be noted that in the FLAC3D 6.0 software, the maximum principal stress and the minimum principal stress are distinguished by numerical values (rather than absolute values). Although the stress contour displayed in the figure is marked with the minimum principal stress, the absolute value of the principal stress is the largest, so the stress in the graph should be the maximum principal stress.

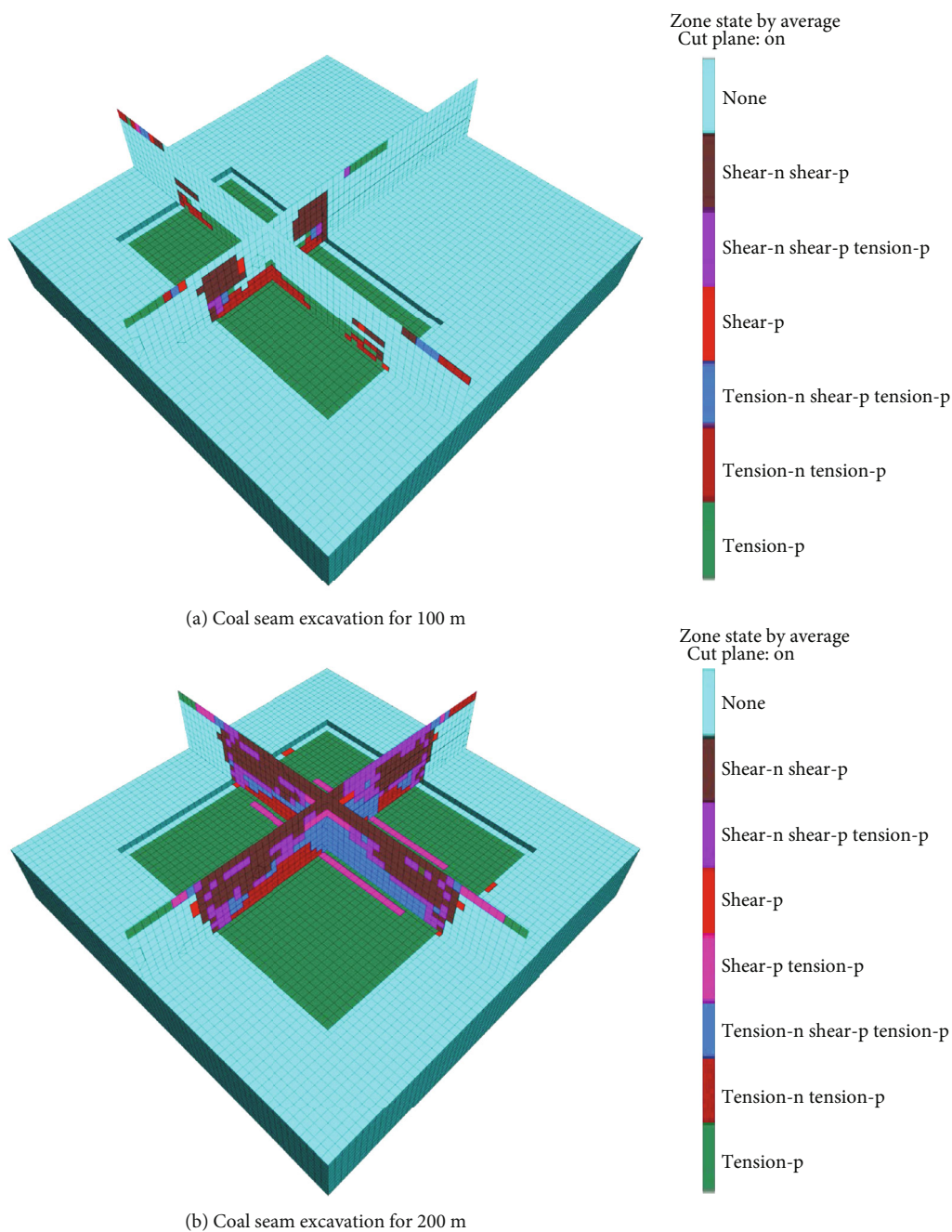


FIGURE 6: Distribution of the plastic zone in the standard model.

TABLE 2: Mechanical parameters of the roof, coal seam, and floor in the model with rockburst tendency.

Lithology	Thickness/ m	Bulk modulus/ GPa	Shear modulus/ GPa	Cohesive force/ MPa	Tensile strength/ MPa	Friction angle/°	Density Kg/m <sup>3</sup>
Sandstone	19.0	2.23	1.74	8.2	1.86	48	2839
Coal	5.0	1.41	0.45	2	1.6	35	1400
Mudstone_ 2	9.0	1.76	0.61	5.2	1.0	40	2762

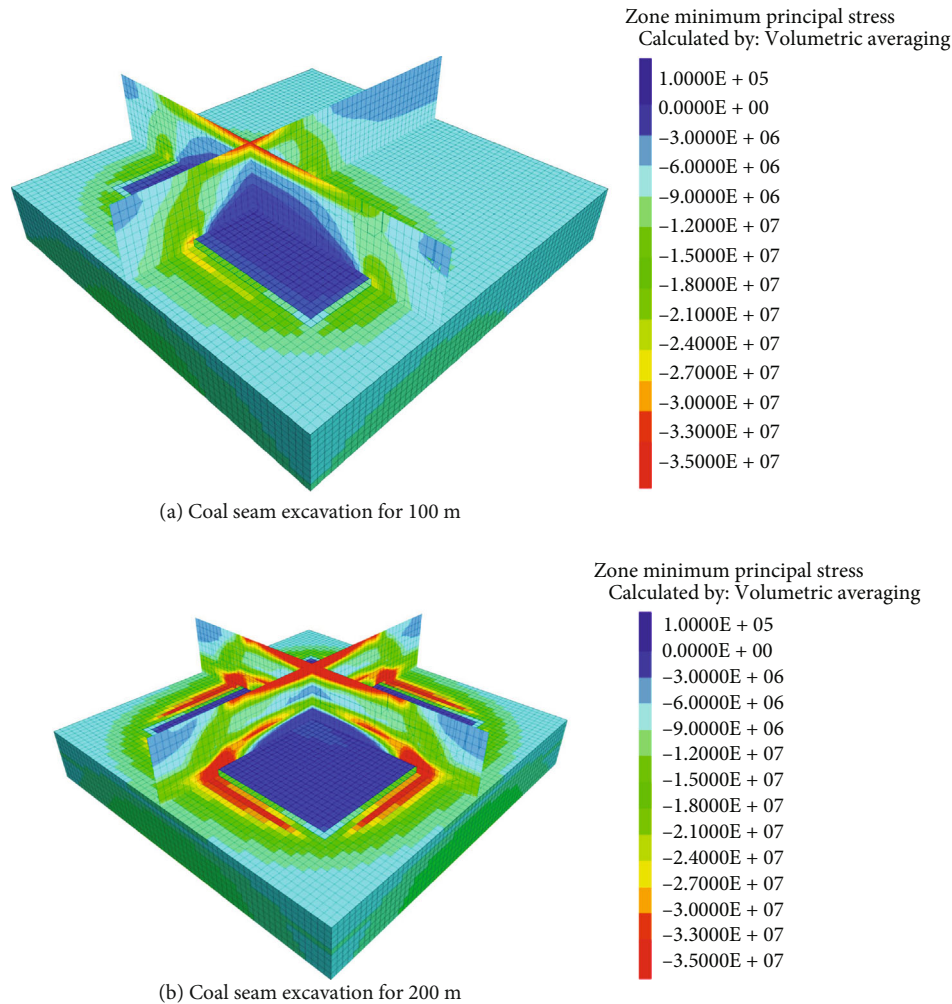


FIGURE 7: Distribution of maximum principal stress when mining coal stratum with rockburst tendency.

Figure 5 shows the distribution of the maximum principal stress in the standard mining model. To reflect the distribution of the maximum principal stress from multiple perspectives, multiple slices are selected to display the distribution of the stress contour. The bottom surface in Figure 5 is the coal seam, and the mining space is formed after excavation. The other two slices are taken from the middle of the excavation space and the model, respectively, to show the stress distribution of the model along with the parallel and vertical mining directions.

It can be seen from Figure 5 that after the coal seam is mined for 100 m, low-stress zones are formed on the bottom and the roof of the coal seam, while stress concentration zones are formed around the excavation space. In the horizontal direction, the stress concentration area is mainly distributed within 5-10 m of the working face and the surrounding coal pillars, and the maximum stress is about 27 MPa; in the vertical direction, the high-stress area is distributed in the middle of the mining space 40 m above the working face with the maximum value of 35 MPa. After the coal seam is mined for 200 m, the mining space is further expanded, and the degree of stress concentration and the distribution range of high-stress areas are further increased.

In the horizontal direction, the high-stress area is still distributed within 5-10 m of the working face and the surrounding coal pillars, but the maximum value can reach about 35 MPa; in the vertical direction, the distribution range of the high-stress area is further expanded, and the maximum stress can reach more than 35 MPa. Calculated with the original rock stress of 9 MPa, the stress concentration coefficient in the horizontal direction is increased from the original 3 to 4 with the working face advancing. The stress concentration degree is significantly improved.

*3.1.3. Distribution of Plastic Zone in the Standard Mining Model.* Figure 6 shows the distribution of the plastic zone in the standard mining model. Similar to the stress distribution, several slices are selected to show the distribution of the plastic zone. After the coal seam is mined for 100 m, the tensile stress plastic zone is formed in the coal seam floor after excavation in the horizontal direction. In the vertical direction, the tensile-shear composite failure occurs in the middle of the mining space, and the upper part of the excavation boundary of the working face is dominated by the shear plastic zone. The current distribution range of the plastic zone is not large, and the range of these plastic zones reflects



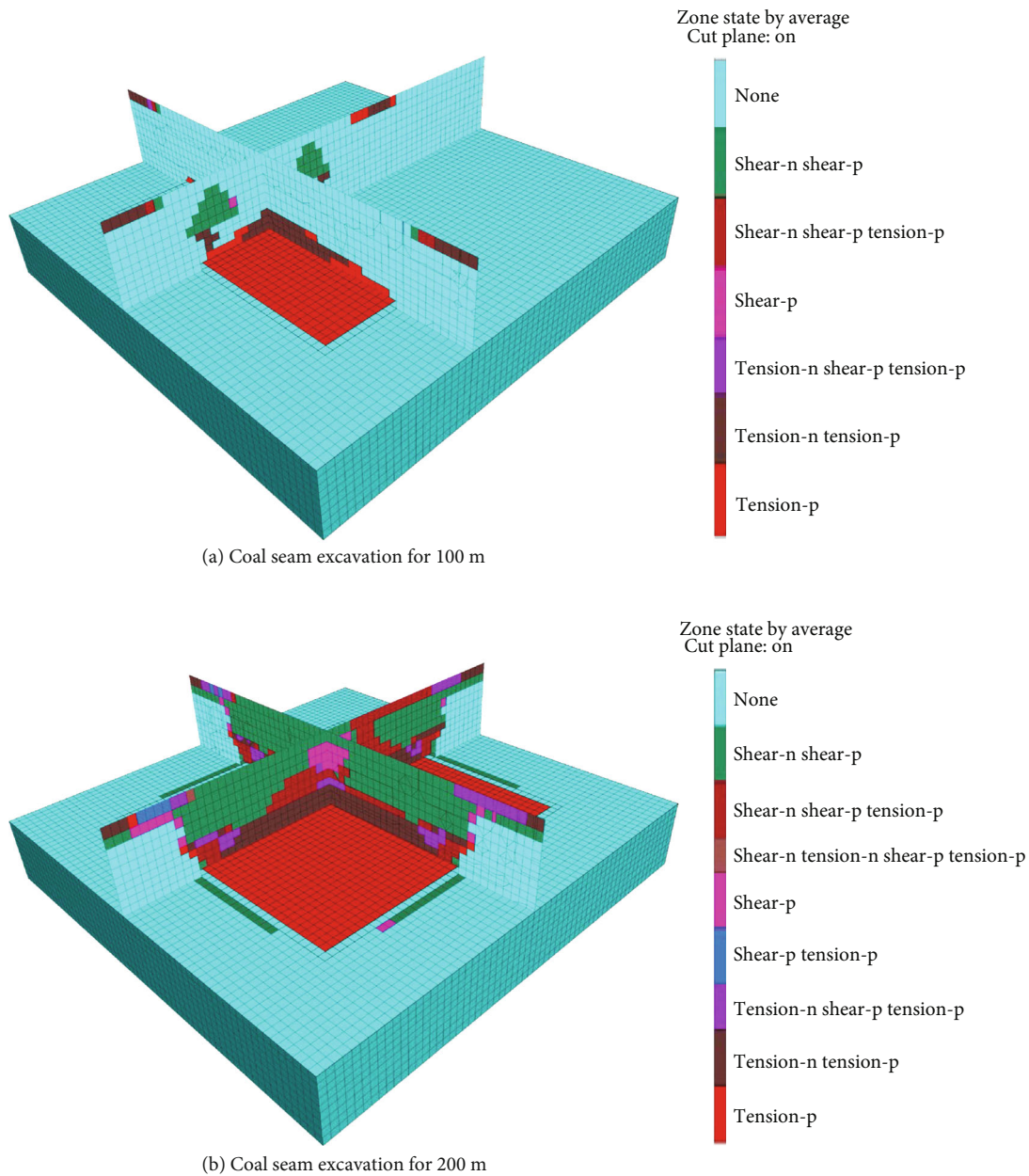


FIGURE 8: Plastic zone distribution during mining of a coal seam with rockburst tendency.

the current distribution of the low-stress zone. After the coal seam is mined for 200 m, the mining space is further expanded and the distribution range of the plastic zone is further increased. In the horizontal direction, the bottom of the coal seam is still dominated by the tensile plastic zone, while in the vertical direction, the overlying strata of the mining space have almost completely formed the plastic zone. The increase of the mining space leads to the formation of an obvious plastic zone in the position where the roof is suspended in a large area, and the load-bearing capacity of this area is lost.

**3.2. Simulation of Mining Coal and Rock Formations with Rockburst Tendency.** In the standard model in Section 3.1, the coal and roof and floor rock formations in the model

have no rockburst tendency. In this section, the established model takes into account the rockburst tendency of coal and rock for comparison. There are four parameters to describe the rockburst tendency, among which the uniaxial compressive strength is the most critical indicator to describe the rockburst tendency. In the Mohr-Coulomb criterion, the shear strength of rock is determined by cohesion and internal friction angle. Apart from the shear failure, tensile failure is also a common failure mode of rock during the rock failure process. Therefore, the parameter of tensile strength cannot be ignored in addition to the above two parameters. Then the rock strata whose rockburst tendency should be increased are considered. Since the location of rockburst is generally located in the coal seam, the adjacent roof and floor, the three mechanical parameters of these

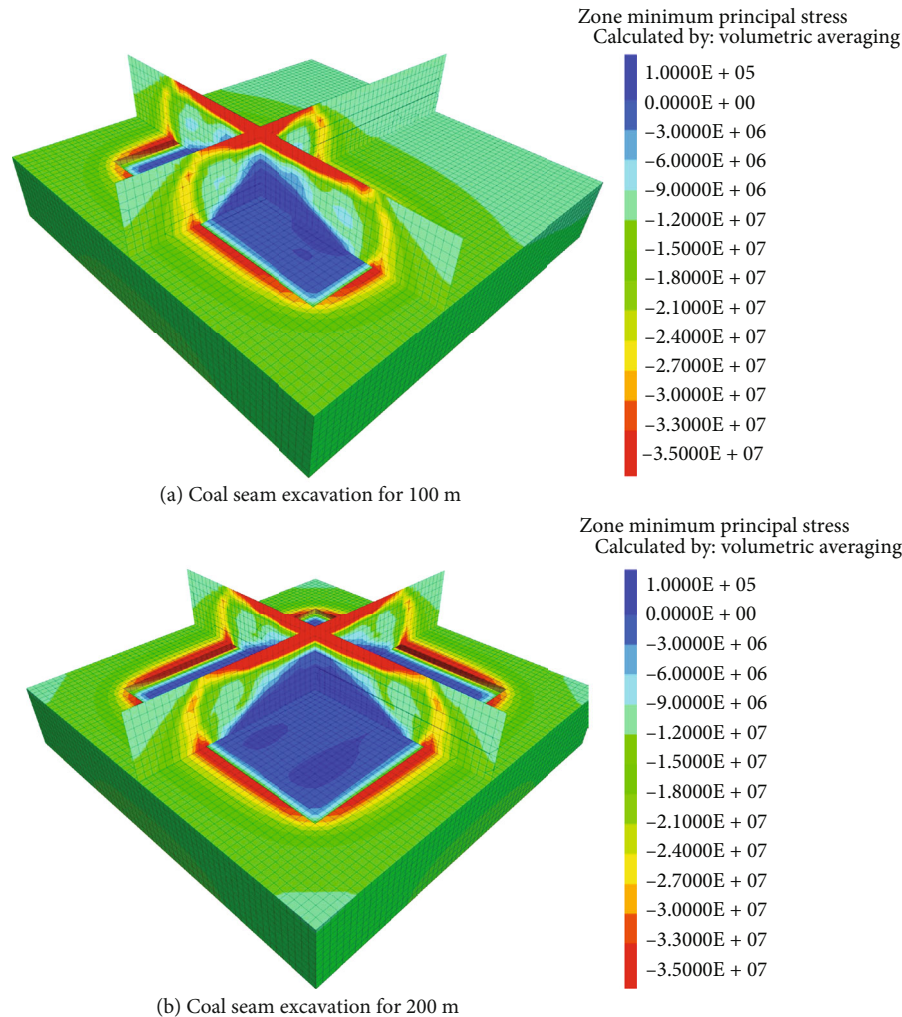


FIGURE 9: Maximum principal stress distribution with a buried depth of 500 m.

three strata are increased. In this way, the rockburst tendency of coal, roof, and floor strata is improved to study the influence of rockburst tendency on the distribution of the maximum principal stress and plastic zone during the mining process. Table 2 shows the mechanical parameters of the coal seam, the mudstone<sub>2</sub>, and the sandstone used in this model. The mechanical parameters of the remaining rock formations are the same as those in Table 1.

**3.2.1. Stress Distribution when Mining the Coal Seam with Rockburst Tendency.** Figure 7 shows the distribution of the maximum principal stress when mining a coal seam with rockburst tendency. The situation of the maximum principal stress contour in Figure 7 is very similar to that in Figure 5. But some differences should be noted. One point is that the high stress in the horizontal direction tends to transfer to the deep zone. After the coal seam is excavated for 100 m, the high stress in the coal seam is concentrated in the range of 10-15 m in front of the coal seam. This trend is more obvious after the coal seam is mined for 200 m, and it can be seen that the stress concentration occurs in the range of 15-20 m in front of the coal seam. The second point is the reduction in the extent of the low-stress zone in the vertical direction.

It can be seen that after the working face is mined for 200 m, the low-stress area in Figure 7(b) is significantly smaller than that in Figure 5(b), and the high-stress areas in the horizontal and vertical directions are connected. It can be found that although the value of the maximum principal stress and the stress concentration coefficient does not change much, the stress distribution in this model is significantly different from the standard model. This is because the energy storage capacity of the rock strata with high bearing capacity is improved, and stress concentration has already formed in the shallow part of the excavation. Therefore, rockbursts often occur when mining the coal seam with rockburst tendency.

**3.2.2. Plastic Zone Distribution when Mining the Coal Seam with Rockburst Tendency.** Figure 8 shows the plastic zone distribution during mining of a coal seam with rockburst tendency. The differences in the distribution of the plastic zone in Figure 6 are as follows. The first is that the scope of the plastic zone of the roof near the mining space is decreasing. This can be seen by comparing Figures 6(a) and 8(a). In Figure 6(a), most of the surrounding rock above the working face has become a plastic zone. However, in

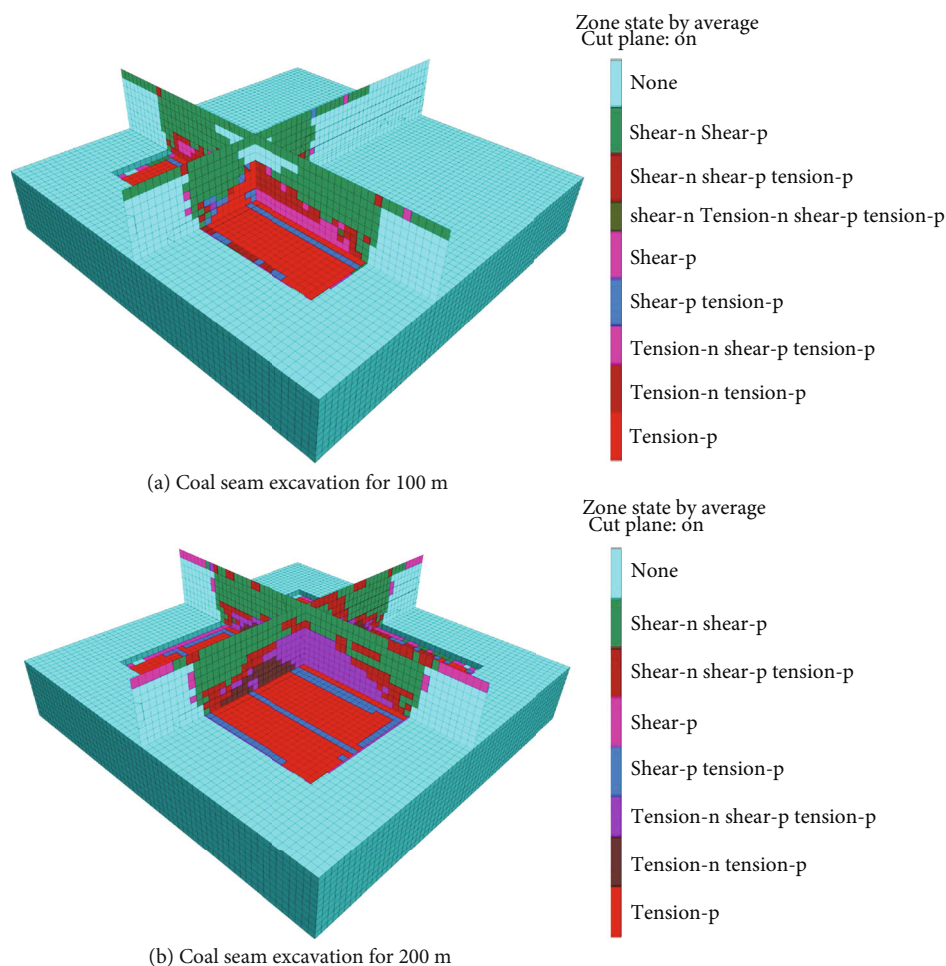


FIGURE 10: Distribution of plastic zone when buried depth is 500 m.

Figure 8(a), only some elements above the working surface are still in the elastic state. The second is that the model shows the characteristics of partition damage. It can be seen in Figure 8(b) that a plastic zone appears around the working face in the horizontal direction separated by elastic elements. The interlacing of the elastic and plastic zone cuts off the integrity of the rock formation, which is not conducive to the development of the overall bearing capacity of the rock formation and easily leads to the dynamic failure of the rock formations.

**3.3. Simulation of Coal Mining under High Stress.** In Section 3.3, the established model focuses on considering the influence of high stress. In the model established in this section, the thickness of the overburden strata is increased from 300 to 500 m. In this way, the distribution of the maximum principal stress and the plastic zone in the coal seam mining process is simulated under a high-stress environment.

**3.3.1. Stress Distribution of Coal Seam Mining after Increasing Burial Model Depth.** Figure 9 shows the maximum principal stress distribution during coal mining with increased burial model depth. Compared with the maximum principal stress distribution in the standard mining model, the maximum principal stress distribution after the burial

depth increases to 500 m presents the following new characteristics. First, the overall stress level in the space affected by mining activities has increased significantly. It can be seen that the original rock stress in this model is close to 15 MPa. Except for the tensile stress area, there is almost no 0-9 MPa compressive stress in the coal seam plane. Second, the range of high-stress distribution also increases significantly. It can be seen from Figure 9 that after the coal seam is excavated for 100 m, the area with the maximum principal stress exceeding 35 MPa almost exceeds the range of the standard model with an excavation length of 200 m. Under the condition that the strength of the coal and rock strata remains unchanged, the increase in the stress level would cause the coal and rock masses to be more easily damaged, and the damage process would become more severe.

**3.3.2. Plastic Zone Distribution of Coal Seam Mining after Increasing Burial Model Depth.** Figure 10 shows the distribution of the plastic zone when the model is buried at a depth of 500 m. With the large increase in the stress level, the extent of the plastic zone of the model increases significantly in both the horizontal and vertical directions. After the coal seam is mined for 100 m, plastic elements have appeared in the coal pillar area in the horizontal direction, and a large-scale shear plastic zone has appeared in the overlying rock

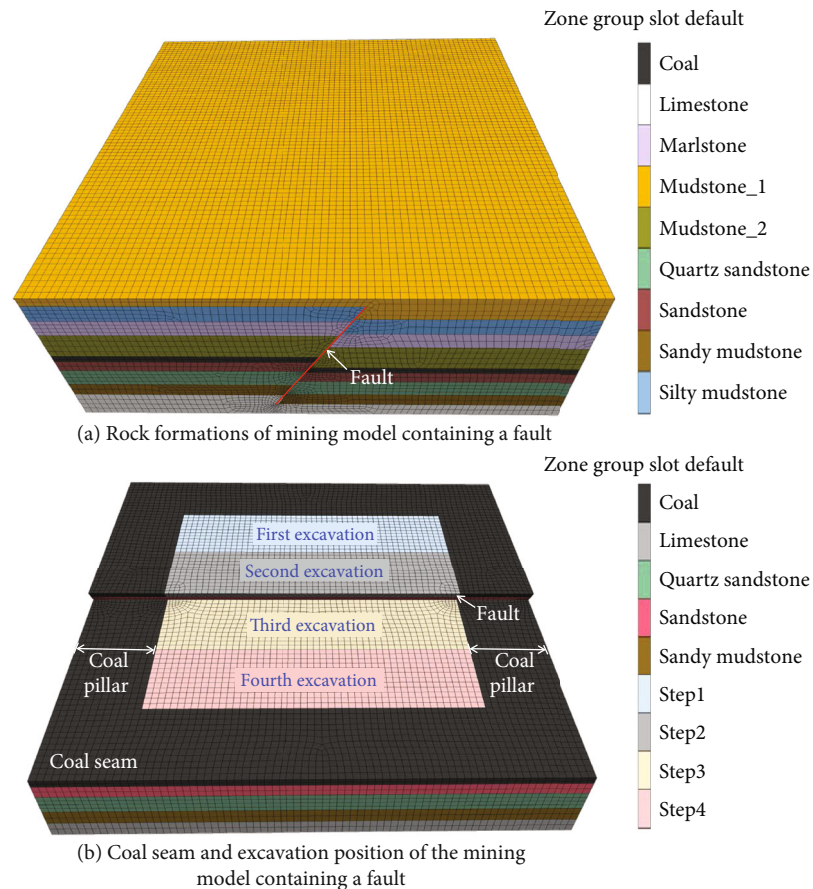


FIGURE 11: Established mining model with a fault.

in the horizontal direction. After the coal seam is excavated for 200 m, the expansion trend of the plastic zone is more obvious. Under the high-stress environment, the rock elements change from elastic to a plastic state earlier, and the bearing capacity of coal pillars and roofs is greatly weakened.

**3.4. Simulation of the Mining Model Containing Fault Structures.** In this section, the mining model contains a fault plane to simulate the distribution of stress and plastic zones under the influence of geological structure. The established model with a fault is shown in Figure 11. The fault is located in the middle of the model and runs through 7 rock formations (except the mudstone at the top and the limestone at the bottom). The dip angle of the fault is  $60^\circ$  with a vertical height difference of 10 m. The mechanical parameters of all rock formations are the same as in Table 1.

**3.4.1. Stress Distribution in the Mining Model with a Fault.** Figure 12 shows the maximum principal stress distribution during the coal mining process of the model containing a fault. Compared with Figure 5, three points are worth noting. First, the magnitude of the maximum principal stress in the horizontal direction is slightly reduced, and the range of high-stress distribution is somewhat reduced, especially when the working face is excavated for 100 m. Second, the stress concentration degree directly above the mining face is reduced. It can be seen from Figure 12(b) that a small local

high-stress area directly above the working face becomes a larger local subhigh stress area. Third, stress concentration occurs on the fault plane. As shown in Figure 12(c), stress concentration is formed on both sides of the fault plane and the lower-middle position, while an obvious tensile stress concentration zone is formed in the middle position of the fault plane. This indicates that the fault may cut off the transmission of mining stress, resulting in the stress reduction of surrounding rock around the working face. However, new stress concentration areas could be formed near the fault plane, and the existence of these areas makes the fault very easy to slip under the influence of mining. Therefore, the stability of the structure around the fault caused by mining should be more concerned for a mining model with a fault.

**3.4.2. Distribution of the Plastic Zones in the Mining Model with a Fault.** Figure 13 shows the distribution of plastic zones when mining the model with a fault. Under the influence of the fault plane, the extent of the plastic zone, especially the shear plastic zone, is greatly increased. After excavation for 100 m, a certain range of shear plastic zone appears in the coal pillar area on the horizontal plane; in the vertical direction, the range of the shear plastic zone is greatly increased above the rock layer near the fault plane. After the coal seam is excavated for 200 m, the expansion trend of the shear plastic zone near the fault plane is more

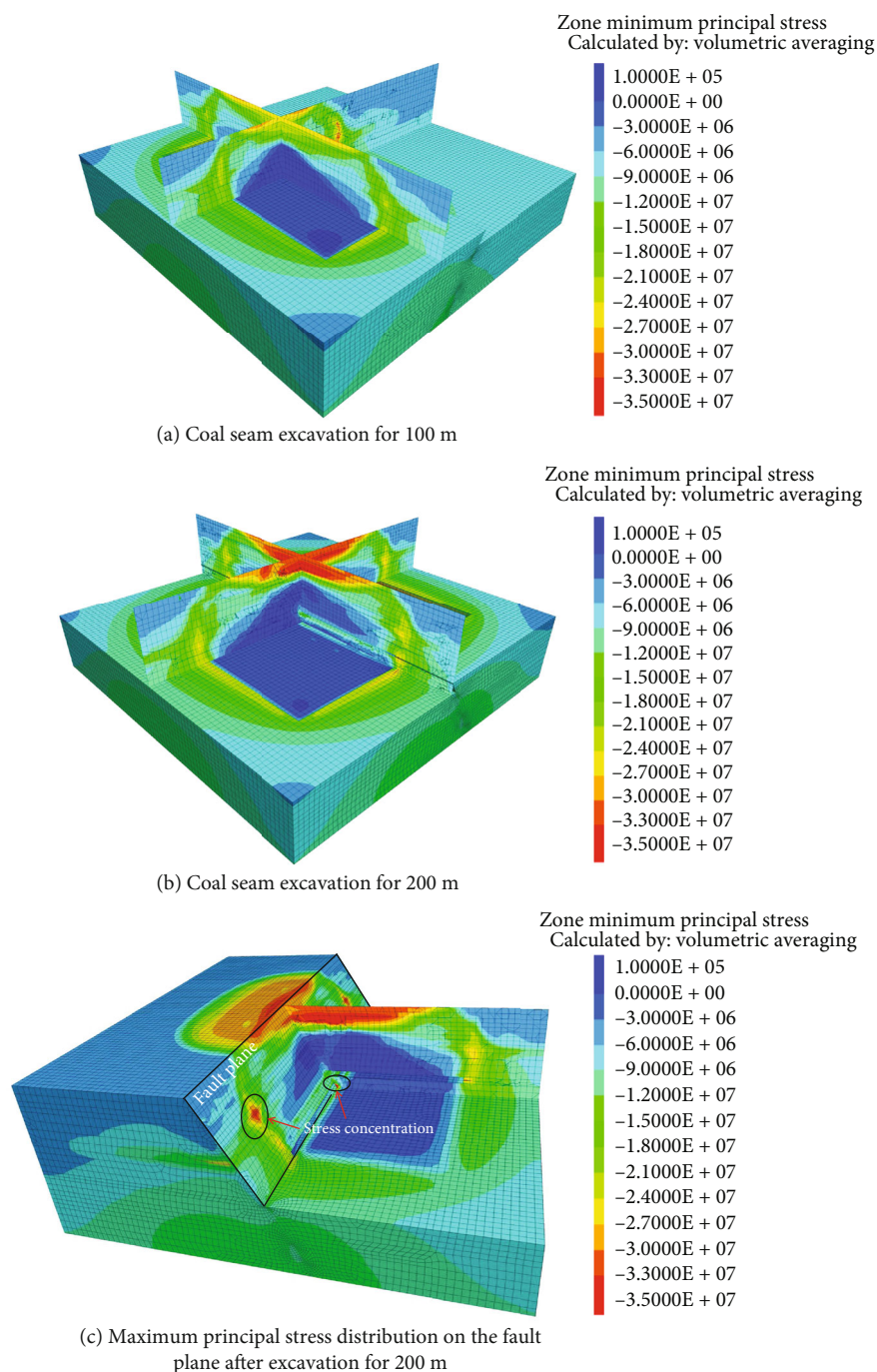


FIGURE 12: Maximum principal stress distribution of the mining model with a fault.

obvious, and the area of the plastic zone located above the coal pillar expands more significantly. The presence of the fault reduces the overall stability of surrounding formations, and shear-slip failure is becoming the dominant mode of failure type of the elements near the fault.

#### 4. Quantitative Evaluation Method of Coal Rockburst Risk

Quantitative evaluation of rockburst risk has always been the focus of dynamic disaster research in coal mines. There are

two quantitative evaluation methods for rockburst risk. One method is based on the geological structure, mining factors, and other geological information, using multivariate statistical analysis to complete the comprehensive analysis of rockburst risk. This method mainly evaluates the rockburst risk before mining; one of the typical methods is the comprehensive index method. However, the geological information of coal mines cannot be fully obtained before mining, which leads to the mechanical effect under the influence of geological factors that could not be reasonably described. Therefore this method is still subjective in the quantitative evaluation of rockbursts.

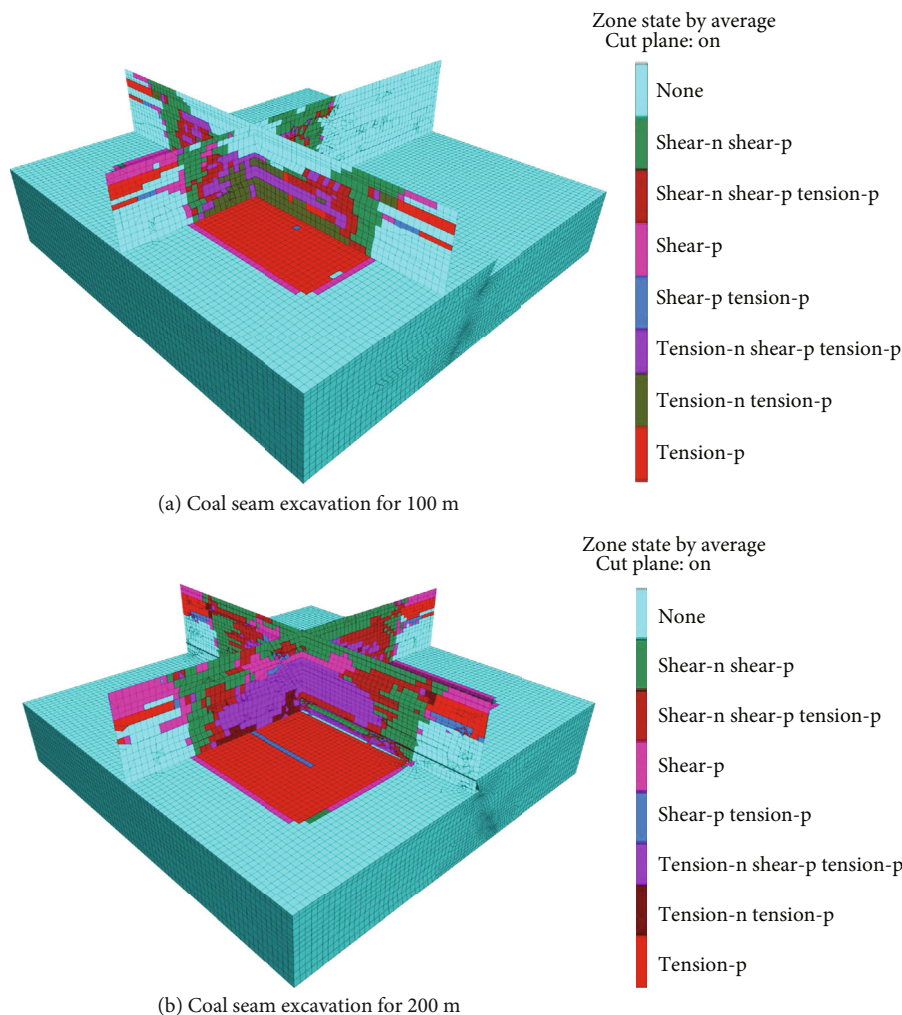


FIGURE 13: Distribution of plastic zone of the mining model with a fault.

The other method relies on digital information such as microseismic and in situ stress and carries out early warning based on the evolution characteristics of monitoring data, which is mainly for the evaluation of rockburst risk in coal mining. Different types of monitoring data are indirect descriptions of specific stress states, which have the same essence. Hence, this method is the main direction of quantitative evaluation of rockburst risk at present. Quantitative evaluation of rockburst risk has always been the focus of dynamic disaster research in coal mines. A suitable evaluation method should reflect the contribution of material, stress, and structural factors to rockbursts. The physical quantity that best reflects the risk of rockbursts is energy. The locations with high energy accumulation generally have a higher rockburst tendency and are generally accompanied by high-stress concentrations. Microseismic monitoring is a good tool to obtain energy release [39]. In this section, the microseisms are classified into a separate category as a regional coverage method. Daily microseismic frequency is regarded as the most reliable indicator of rockburst risk.

**4.1. Proposal for a Quantitative Evaluation Method.** The release of microseismic signals in the mining process reflects

the energy release of rock materials, the appearance of stress superimposition effects, and the activation of large geological structures. Microseismic signals can be considered as the parameters that comprehensively reflect the risk of rockburst. Although microseismic monitoring is an effective means to evaluate rockbursts, the absence of microseismic signals does not mean that there are no rockbursts. This point of view can be supported by a rockburst case. A rockburst accident occurred in a coal mine in Shandong Province in 2012, resulting in two deaths. The excavation of the nearby working face had been stopped one day before the rockburst accident, and no microseismic signal was monitored before the accident [19]. According to the data analysis of the daily frequency of microseisms, statistical methods classify the risk levels. The primary basis is that, for a specific system, the time it is in a normal state would account for the vast majority of its total running time, and the numerical frequency of a specific index that has a causal relationship with the system operation is counted. The numerical range with the most significant proportion is the standard range describing the normal state of the system.

According to the central limit theorem, the distribution of the random variable sequence is asymptotically normal.

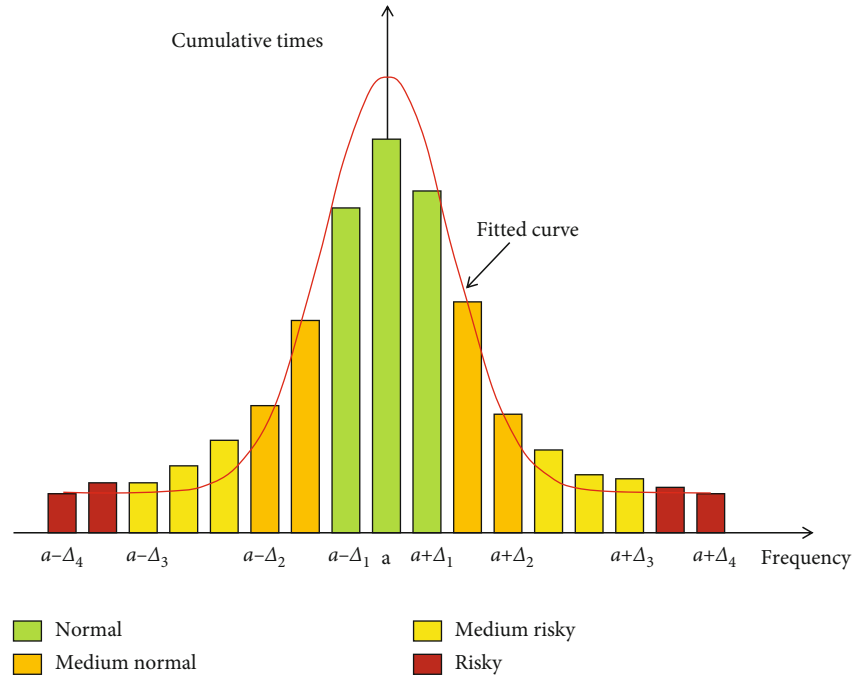


FIGURE 14: Classification of rockburst risk.

The central limit theorem is the most important theorem in the probability theory, with a wide range of practical application backgrounds. Some phenomena are affected by many independent random factors. If the influence of each factor is minimal, the total influence can be regarded as obeying a normal distribution. Under this concept, the normal distribution function in statistics describes the probability density of different daily occurrences of microseisms. The probability density function of the normal distribution is shown.

$$f(x) = \frac{1}{\sqrt{2\pi}b} \exp \left[ -\frac{(x-a)^2}{2b^2} \right], \quad (1)$$

where  $b$  represents the expectation of this set of variables and  $a$  represents the standard deviation of this set of variables.

When using this method for risk evaluation, the probability density function and curve must first be fitted according to the statistical data of the microseismic signal. According to the probability density curve, the closer to the central axis of the curve, the higher the frequency of data occurrence and the more regular the data is. The farther away from the central axis of the curve, the lower the frequency of data occurrence and the more abnormal the data is. According to the fitted curve, the abnormal conditions with more and fewer microseisms are determined, and these two types of conditions are used as an important basis for predicting the risk of rockburst. Finally, four levels are divided: normal, medium normal, medium risky, and risky. Figure 4 shows the classification of rockburst risks.

According to Figure 14, the rockburst risk classification is established in Table 3. The rockburst risk level is classified

TABLE 3: Criteria for classification of risk levels.

Range	Risk level
$(a - \Delta_1 \sim a + \Delta_1)$	Normal
$(a - \Delta_2 \sim a - \Delta_1) \cup (a + \Delta_1 \sim a + \Delta_2)$	Medium normal
$(a - \Delta_3 \sim a - \Delta_2) \cup (a + \Delta_2 \sim a + \Delta_3)$	Medium risky
$(a - \Delta_4 \sim a - \Delta_3) \cup (a + \Delta_3 \sim a + \Delta_4)$	Risky

by the expectation of the microseismic frequency  $a$ , and the degree of deviation of the microseismic frequency from the expectation,  $\Delta_1, \Delta_2, \Delta_3$ , and  $\Delta_4$ . The degree to which the frequency of microseisms deviates from the expectation reflects the probability of the number of microseisms with that frequency. Therefore, it is also possible to replace the interval of the microseismic frequency with a probability interval. For different mines, the corresponding  $\Delta_1, \Delta_2, \Delta_3$ , and  $\Delta_4$  can be set to classify the rockburst risk level considering the conditions of the mine.

What needs to be emphasized are the application conditions of this model. The normal distribution model is a distribution model for random variables. The premise of this model is that many factors affecting the daily microseismic frequency are independent of each other. Under normal mining conditions, the frequency of daily microseisms meets the requirements of randomness, but this random variable is affected by artificial mining activities. For instance, in the case where a working face is stopped, the microseismic signals of this coal mine are likely to be absent; then, the microseismic frequency during this time is low and may deviate too far from the average value, but it is unreasonable to judge that this coal mine has the risk of rockbursts.

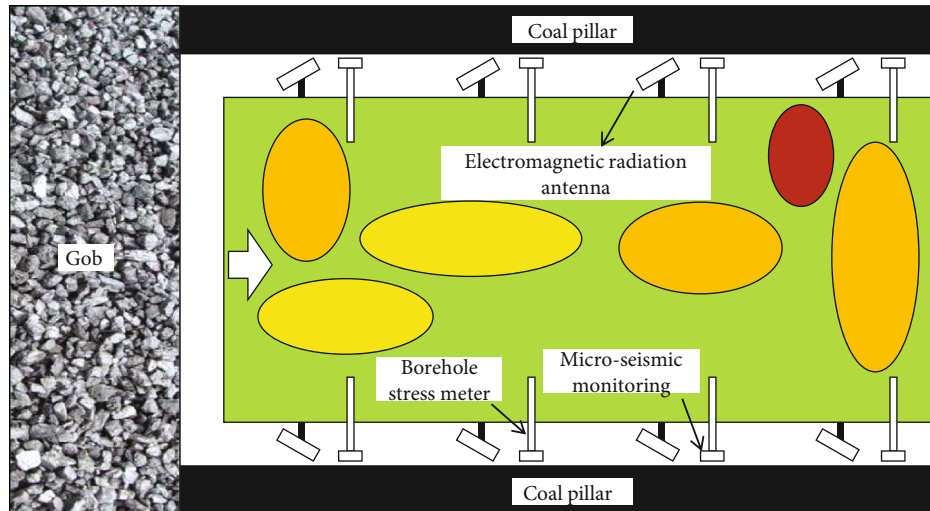


FIGURE 15: Schematic result of partial area division.

Therefore, when using this evaluation model, it is necessary to ensure that the mining process is carried out in a normal, ordered state. The collection of data in this model should be that the artificial mining conditions are consistent within a certain period.

**4.2. Division of Rockburst Risk Area.** For local monitoring methods such as stress and electromagnetic radiation, the main features of local coverage are used to support the specific division of rockburst risk areas and not forcibly integrated into the overall risk evaluation of the working face. This method is mainly based on long-term on-site observation: most coal mines are equipped with multiple monitoring methods, and multiple sensors are usually installed in local areas. For a local area, although the data volume of a single sensor is limited, the increase in data types can make up for the lack of a single data volume to achieve a reliable evaluation of the local area. Based on the specific arrangement of sensors, on the premise that each local area contains more than 3 data sources (different types of data sources are recommended), the working surface is divided according to the location of the measuring points, as shown in Figure 15.

For the integration of monitoring means, the principle of “one hole for multiple uses” should be adopted, and the space occupied by the monitoring means should be minimized on the premise of ensuring the effectiveness of each monitoring means. The data fusion algorithm can be implemented using mature algorithms such as hierarchical analysis, neural networks, and Bayesian estimation. It needs to be emphasized that the quantitative evaluation of rockburst risk does not mean the complexity of methods or indicators. Appropriate operating thresholds should also be included in the quantitative evaluation considerations. If the authenticity and validity of the data are met, it can be considered in the quantitative evaluation category. The above methods rely on raw data and are still applicable when breakthroughs are made in fundamental theories or detection methods.

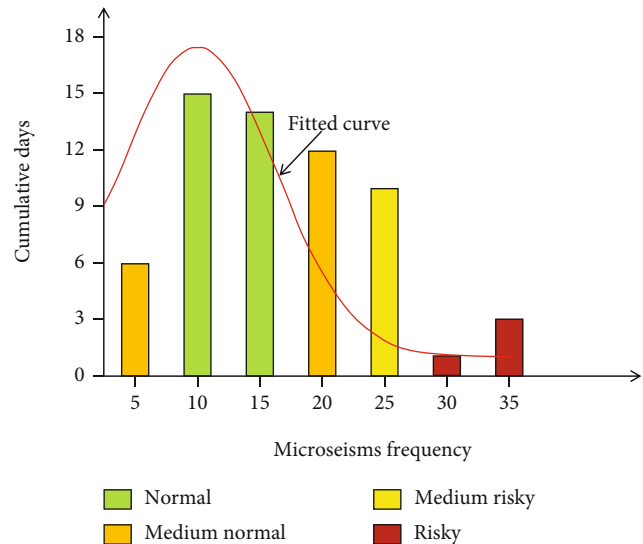


FIGURE 16: Rockburst evaluation by statistics of daily microseismic frequency.

**4.3. Engineering Example of Quantitative Evaluation of Rockburst.** Da’anshan Coal Mine is located in the mountainous area in western Beijing, and its geological structure and stress environment are highly complex. The mine attaches great importance to rockburst prevention and control and is equipped with comprehensive monitoring equipment, including microseismic, borehole stress gauge, and electromagnetic radiation. The daily frequency of microseismic monitoring with regional coverage capability is statistically analyzed for microseismic events from September 1 to October 31, 2018. The statistical results are shown in Figure 16.

It can be seen from Figure 16 that 5 to 10 microseismic events occur most frequently in this period. The probability density curve of the normal distribution is established. Local area division is completed based on sensor distribution for stress and electromagnetic radiation monitoring with local



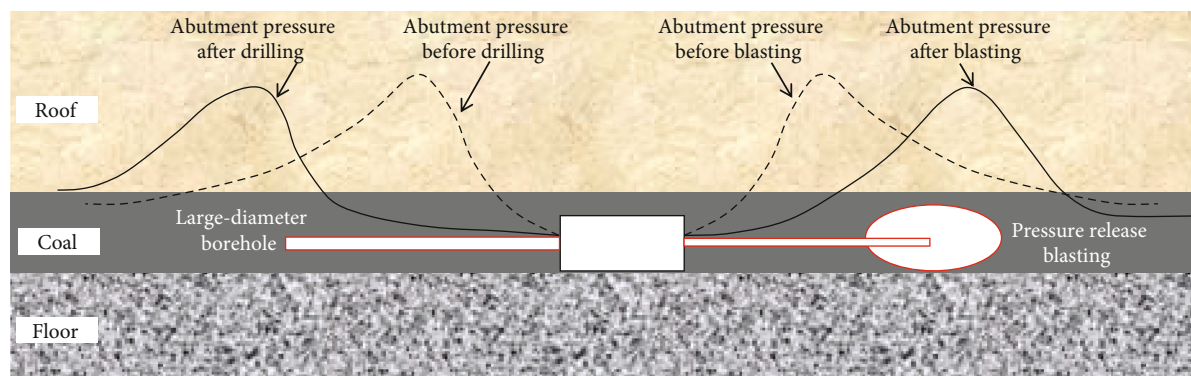


FIGURE 17: Principle of coal seam pressure relief technology.

coverage capabilities. As data fusion involves many calculations, the data is fused by the analytic hierarchy process, and the results of the fusion of different local area normalization complete the division of relative risk levels in each local area of the working face. With the support of the abovementioned quantitative evaluation method of rockburst risk, mining activities in Da'an Shan Coal Mine were kept safe.

## 5. Discussion

The role of the three factors in inducing rockbursts and the expectation of rockbursts evaluation are discussed in this section. The essence of rockbursts is the phenomenon that mining activities lead to stress concentration, which triggers large-scale energy release. The studies of many scholars have shown that rockbursts could occur when mining coal seams are with or without rockburst tendency. The same goes for geological structures. The rockburst tendency of the material and the existence and distribution trend of faults all play a role through stress in the final analysis. This can be seen from the current rockburst prevention technology in coal mines. Figure 17 shows the principle of large-diameter borehole pressure relief and coal seam pressure relief blasting technology. Coal seam pressure relief technology is a local prevention and control method of rockbursts based on stress control theory. Its essence is to implement pressure relief measures on the current or potential stress concentration area in the coal seam to release the high stress and transfer stress to the deep part of the coal seam, thereby reducing the rockburst risk of the coal seam. Commonly-used coal seam pressure relief technologies include large-diameter borehole pressure relief technology and coal seam pressure relief blasting technology. In the former method, a crushing zone is formed around the drilling hole by constructing large-diameter drilling holes, and the crushing zones adjacent to the drilling hole penetrate each other. The brittleness and elastic energy accumulation capacity of the coal seam are greatly weakened, thereby reducing the stress concentration of the coal seam in the construction area. The latter method uses deep-hole blasting to relieve the internal pressure of the coal body in the gang to reduce the rockburst risk of the coal seam. After blasting, the stress concentration of the shallow coal on both sides decreases, and the stress peak

shifts to the deep coal seam. The gravity of the overlying strata is carried by the deep coal bearing three-dimensional stress. Therefore, the core factor among the three factors should be the stress factors. Controlling the stress is the key to controlling the rockbursts in coal mines, and monitoring the stress is the key to early warning and prevention of rockbursts.

According to the above analysis, the most direct and effective method for the evaluation and early warning of rockburst should be stress monitoring. However, stress monitoring technology has not made a remarkable breakthrough in recent years. At present, stress monitoring methods mainly include the stress recovery method, stress relief method, and hydraulic fracturing method, but the data obtained by any method is the stress at a certain position and time. How to obtain continuous stress data in time and space is the development direction of stress monitoring. Given the deficiency in stress monitoring, using microseismic monitoring to quantitatively evaluate the risk of rockbursts is a compromise solution. Although the effect of microseismic on rockburst prediction and prevention is limited, however, the microseismic signal reflects the release of energy, the factor most related to stress, so the role of microseismic monitoring in the short term cannot be replaced. In the future, the monitoring system combining microseisms with stress is the direction to accurately and quantitatively evaluate the rockburst risk.

## 6. Conclusions

A multifactor analysis and quantitative evaluation method for rockburst risk in coal mines is proposed in this study. Theoretical analysis, multifactor numerical simulation, and establishment of the rockburst evaluation model are carried out. The following conclusions are obtained.

- (1) The mechanism of rockbursts in coal mines under the action of rock material, stress environment, and large geological structure is described in detail, including energy evolution characteristics during the loading process of different rock media, the destruction mechanism of the surrounding underground rock under the combined action of dynamic

and static loads, and pillar rockburst triggered by the activation of large-scale geological structures

- (2) Based on a standard mining model, three comparative models considering the rockburst tendency of coal and rock formations, high stress, and fault planes are established. The distribution of maximum principal stress and plastic zone during the mining process is compared. Under the same model standard, the reasons why the above three types of factors are easy to cause rockbursts in coal mines are revealed
- (3) A normal distribution function based on the frequency of daily microseisms is established. This function is used to judge whether the number of microseisms is abnormal, and then to judge the rockburst risk of coal mines, making a new exploration for the quantitative evaluation of rockbursts in coal mines

### Data Availability

All data, models, or code generated or used during the study are available from the corresponding author by request.

### Conflicts of Interest

The authors declare that they have no conflict of interest.

### Acknowledgments

This study is supported by the National Natural Science Foundation of China (No. 52104090), the Open Research Fund Program of State Key Laboratory of Hydroscience and Engineering (No. sklhse-2021-C-06), the Special Projects of Science and Technology Innovation Entrepreneurship Funds by China Coal Technology Engineering Group (Nos. 2022-MS003, 2019-2-ZD001).

### References

- [1] P. Konicek, K. Soucek, L. Stas, and R. Singh, "Long-hole distress blasting for rockburst control during deep underground coal mining," *International Journal of Rock Mechanics and Mining Sciences*, vol. 61, pp. 141–153, 2013.
- [2] Y. Jiang, Y. Zhao, H. Wang, and J. Zhu, "A review of mechanism and prevention technologies of coal bumps in China," *Journal of Rock Mechanics and Geotechnical Engineering*, vol. 9, no. 1, pp. 180–194, 2017.
- [3] Y. Zhao, H. Wang, S. Liu, Z. Mu, and Z. Lu, "Dynamic failure risk of coal pillar formed by irregular shape longwall face: a case study," *International Journal of Mining Science and Technology*, vol. 28, no. 5, pp. 775–781, 2018.
- [4] C. Newman and D. Newman, "Numerical analysis for the prediction of bump prone conditions: a southern Appalachian pillar coal bump case study," *International Journal of Mining Science and Technology*, vol. 31, no. 1, pp. 75–81, 2021.
- [5] Y. Pan and L. Dai, "Theoretical formula of rock burst in coal mines," *Journal of China Coal Society*, vol. 46, p. 789, 2021.
- [6] W. Cai, X. Bai, G. Si, W. Cao, S. Gong, and L. Dou, "A monitoring investigation into rock burst mechanism based on the coupled theory of static and dynamic stresses," *Rock Mechanics and Rock Engineering*, vol. 53, no. 12, pp. 5451–5471, 2020.
- [7] M. Rehbock-Sander and T. Jesel, "Fault induced rock bursts and micro-tremors - experiences from the Gotthard Base Tunnel," *Tunnelling and Underground Space Technology*, vol. 81, pp. 358–366, 2018.
- [8] S. Zhu, Y. Feng, F. Jiang, and J. Liu, "Mechanism and risk assessment of overall-instability-induced rockbursts in deep island longwall panels," *International Journal of Rock Mechanics and Mining Sciences*, vol. 106, pp. 342–349, 2018.
- [9] J. Deng, N. S. Kanwar, M. D. Pandey, and W.-C. Xie, "Dynamic buckling mechanism of pillar rockbursts induced by stress waves," *Journal of Rock Mechanics and Geotechnical Engineering*, vol. 11, no. 5, pp. 944–953, 2019.
- [10] P. Konicek, J. Ptacek, P. Waclawik, and V. Kajzar, "Long-term Czech experiences with rockbursts with applicability to today's underground coal mines," *Rock Mechanics and Rock Engineering*, vol. 52, no. 5, pp. 1447–1458, 2019.
- [11] W. Du, K. Zhang, and H. Sun, "Mechanical properties and energy development characteristics of impact-prone coal specimens under uniaxial cyclic loading," *AIP Advances*, vol. 9, no. 11, article 115114, 2019.
- [12] Y. Zhao and Y. Jiang, "Acoustic emission and thermal infrared precursors associated with bump-prone coal failure," *International Journal of Coal Geology*, vol. 83, no. 1, pp. 11–20, 2010.
- [13] Y. Yu, D.-C. Zhao, G.-L. Feng, D. X. Geng, and H. S. Guo, "Energy evolution and acoustic emission characteristics of uniaxial compression failure of anchored layered sandstone," *Frontiers in Earth Science*, vol. 10, 2022.
- [14] Y. Xue, J. Liu, P. G. Ranjith, F. Gao, Z. Zhang, and S. Wang, "Experimental investigation of mechanical properties, impact tendency, and brittleness characteristics of coal mass under different gas adsorption pressures," *Geomech Geophys Geo-Energy Geo-Resources*, vol. 8, no. 5, p. 131, 2022.
- [15] Y. Di and E. Wang, "Rock burst precursor electromagnetic radiation signal recognition method and early warning application based on recurrent neural networks," *Rock Mechanics and Rock Engineering*, vol. 54, no. 3, pp. 1449–1461, 2021.
- [16] G.-L. Feng, X.-T. Feng, B. Chen, Y. X. Xiao, and Y. Yu, "A microseismic method for dynamic warning of rockburst development processes in tunnels," *Rock Mechanics and Rock Engineering*, vol. 48, no. 5, pp. 2061–2076, 2015.
- [17] R. Jiang and M. Wei, "An improved method of local mean decomposition with adaptive noise and its application to microseismic signal processing in rock engineering," *Bulletin of Engineering Geology and the Environment*, vol. 80, no. 9, pp. 6877–6895, 2021.
- [18] Q. Shan and T. Qin, "The improved drilling cutting method and its engineering applications," *Geotechnical and Geological Engineering*, vol. 37, no. 5, pp. 3715–3726, 2019.
- [19] Q. Qi, H. Li, and X. Li, "Qualitative and quantitative evaluation of impact risk in underground mine," *Coal Science and Technology*, vol. 49, pp. 12–19, 2020.
- [20] Q. Qi, Y. Peng, H. Li, J. Q. Li, Y. G. Wang, and C. R. Li, "Study of bursting liability of coal and rock," *Chinese Journal of Rock Mechanics and Engineering*, vol. 30, pp. 2736–2742, 2011.
- [21] M. Zhai, F. Jiang, Q. Qi, X. S. Guo, Y. Liu, and S. T. Zhu, "Research and practice of rock burst classified control system," *Journal of China Coal Society*, vol. 42, pp. 3116–3224, 2017.

- [22] P. Konicek and J. Schreiber, "Heavy rockbursts due to longwall mining near protective pillars: a case study," *International Journal of Mining Science and Technology*, vol. 28, no. 5, pp. 799–805, 2018.
- [23] B.-R. Chen, X.-T. Feng, Q.-P. Li, R. Z. Luo, and S. Li, "Rock burst intensity classification based on the radiated energy with damage intensity at Jinping II Hydropower Station, China," *Rock Mechanics and Rock Engineering*, vol. 48, no. 1, pp. 289–303, 2015.
- [24] Z. Zhu, H. Zhang, J. Han, and Y. Lv, "A risk assessment method for rockburst based on geodynamic environment," *Shock and Vibration*, vol. 2018, Article ID 2586842, 10 pages, 2018.
- [25] J. Wang, D. B. Apel, A. Dyczko et al., "Investigation of the rockburst mechanism of driving roadways in close-distance coal seam mining using numerical modeling method," *Mining, Metallurgy & Exploration*, vol. 38, no. 5, pp. 1899–1921, 2021.
- [26] M. C. Zhang, "Prediction of rockburst hazard based on particle swarm algorithm and neural network," *Neural Computing and Applications*, vol. 34, no. 4, pp. 2649–2659, 2022.
- [27] Y. Yu, G. Feng, C. Xu, B. R. Chen, D. X. Geng, and B. T. Zhu, "Quantitative threshold of energy fractal dimension for immediate rock burst warning in deep tunnel: a case study," *Lithosphere*, vol. 2021, no. Special 4, p. 1699273, 2022.
- [28] G.-L. Feng, B.-R. Chen, Y.-X. Xiao et al., "Microseismic characteristics of rockburst development in deep TBM tunnels with alternating soft-hard strata and application to rockburst warning: a case study of the Neelum-Jhelum hydropower project," *Tunnelling and Underground Space Technology*, vol. 122, article 104398, 2022.
- [29] J. Wang, P. Liu, L. Ma, and M. He, "A rockburst proneness evaluation method based on multidimensional cloud model improved by control variable method and rockburst database," *Lithosphere*, vol. 2022, no. Special 4, 2021.
- [30] C. Liu, L. Du, X. Zhang, Y. Wang, X. Hu, and Y. Han, "A new rock brittleness evaluation method based on the complete stress-strain curve," *Lithosphere*, vol. 2021, no. Special 4, 2021.
- [31] F. Gong, X. Si, X. Li, and S. Wang, "Experimental investigation of strain rockburst in circular caverns under deep three-dimensional high-stress conditions," *Rock Mechanics and Rock Engineering*, vol. 52, no. 5, pp. 1459–1474, 2019.
- [32] X. Li, C. Li, W. Cao, and M. Tao, "Dynamic stress concentration and energy evolution of deep-buried tunnels under blasting loads," *International Journal of Rock Mechanics and Mining Sciences*, vol. 104, pp. 131–146, 2018.
- [33] S. Wang, X. Li, J. Yao et al., "Experimental investigation of rock breakage by a conical pick and its application to non-explosive mechanized mining in deep hard rock," *International Journal of Rock Mechanics and Mining Sciences*, vol. 122, p. 104063, 2019.
- [34] A. Manouchehrian and M. Cai, "Numerical modeling of rockburst near fault zones in deep tunnels," *Tunnelling and Underground Space Technology*, vol. 80, pp. 164–180, 2018.
- [35] C. Jia, H. Wang, X. Sun, X. Yu, and H. Luan, "Study on rockburst prevention technology of isolated working face with thick-hard roof," *Geomechanics and Engineering*, vol. 20, pp. 447–459, 2020.
- [36] X. Shi, X. Zhang, F. Jiang, H. Wang, and J. Wei, "Study on practice of rockburst accident prevention in multi-seam mining controlled by large fault and hard roof," *Geotechnical and Geological Engineering*, vol. 38, no. 6, pp. 6843–6853, 2020.
- [37] C. Xue, A. Cao, W. Guo, S. Wang, Y. Liu, and Z. Shen, "Mechanism of coal burst and prevention practice in deep asymmetric isolated coal pillar: a case study from YaoQiao Coal Mine," *Shock and Vibration*, vol. 2021, Article ID 3751146, 19 pages, 2021.
- [38] Q. Qi, S. Wang, H. Li, P. Mu, W. Du, and G. Yang, "Stress flow theory for coal bump and its numerical implementation," *Journal of China Coal Society*, vol. 47, pp. 172–179, 2022.
- [39] M. Ge, "Efficient mine microseismic monitoring," *International Journal of Coal Geology*, vol. 64, no. 1-2, pp. 44–56, 2005.